M. Okan and M. Duman. / Hacettepe J. Biol. & Chem., 2024, 52 (6), 319-328, Special Issue

Research Article

Hacettepe Journal of Biology and Chemistry

journal homepage: www.hjbc.hacettepe.edu.tr

Harnessing Molecularly Imprinted Polymers in Surface Plasmon Resonance and Quartz Crystal Microbalance for 17α-Ethinyl Estradiol Detection

17α-Etinil Estradiol Tespiti için Yüzey Plazmon Rezonansı ve Kuartz Kristal Mikrobalansda Moleküler Baskılanmış Polimerlerin Kullanımı

Meltem Okan[1*], Memed Duman[2,*]

[1]METU MEMS Center, Ankara, Turkiye.

[2]Nanotechnology and Nanomedicine Division, Institute of Science, Hacettepe University, Ankara, Turkiye.

ABSTRACT

Estradiol is a critical hormone for reproductive health in both females and males, playing a key role in diagnosing conditions such as menopause, infertility, and certain cancers. However, estradiol, especially in its synthetic form, 17α-ethinyl estradiol (17EE), also represents a significant environmental threat as an endocrine-disrupting chemical (EDC), with serious implications for ecosystems and human health. Despite growing awareness of 17EE's role in water contamination and its potential to disrupt aquatic ecosystems and human endocrine systems, existing detection methods for 17EE are limited. Establishing reliable, rapid, and sensitive biosensors for estradiol detection is thus essential for both environmental monitoring and healthcare. In this study, 17EE-imprinted polymeric nanoparticles (17EE-MIPs) were synthesized using mini-emulsion polymerization and characterized. The synthesized 17EE-MIPs were evaluated using Surface Plasmon Resonance (SPR) and Quartz Crystal Microbalance (QCM) platforms. SPR analysis yielded equilibrium and binding kinetic parameters, with the Freundlich model providing the best fit for the 17EE-MIP based system. Following this, 17EE-MIPs were covalently attached to a QCM crystal, where consecutive 17EE concentrations were tested. Both platforms demonstrated high linearity in detecting low concentrations of 17EE, with detection limits of 11.57 µM and 1.335 µM for SPR and QCM, respectively. These results underscore the potential of using MIPs to develop highly sensitive biosensors for hormone detection, with applications in both environmental and healthcare fields.

Key Words

17-alpha-ethinylestradiol, molecularly imprinted polymers, surface plasmon resonance, quartz crystal microbalance.

ÖZ

Estradiol, hem kadın hem de erkeklerde üreme sağlığı için kritik bir hormondur. Estradiol seviyelerinin izlenmesi, menopoz, kısırlık ve bazı kanser türleri gibi çeşitli durumların teşhisinde yardımcı olabilir. Ayrıca estradiol, ekosistemler ve insan sağlığı üzerinde çeşitli etkileri olan bir endokrin bozucu kimyasal türüdür. Tarımsal akış, kanalizasyon ve endüstriyel atıklar yoluyla çevreye girebilir. Bu iki perspektif göz önüne alındığında, estradiol tespiti için biyosensörlerin geliştirilmesi büyük önem taşır. Bu çalışmada, 17-α-etinilestradiol baskılanmış polimerik nanopartiküller (17EE-MBP) mini-emülsiyon polimerizasyonu kullanılarak sentezlenmiş ve karakterize edilmiştir. Kuartz Kristal Mikrobalans (KKM) analizinden önce, 17EE-MBP Yüzey Plazmon Rezonansı (YPR) ile test edilmiştir. Elde edilen verilerden denge ve bağlanma kinetiği analizleri ile denge izoterm modelleri çıkarılmıştır. Freundlich modeli, 17EE-MBP tabanlı YPR platformunu en iyi şekilde temsil etmiştir. Daha sonra, 17EE-MBP KKM kristaline kovalent olarak bağlanmış ve farklı 17EE derişimleri ardışık olarak test edilmiştir. Her iki sistem de yüksek doğrusal sonuçlar vermiştir. YPR ve KKM sensörlerinin tespit limitleri sırasıyla 11.57 ve 1.335 µM olarak hesaplanmıştır. Burada, iki algılama platformu 17EE-MBP'in performansını doğrulamak için kullanılmış ve düşük konsantrasyonlara yüksek tutarlılıkla tepki verdikleri doğrulanmıştır.

Anahtar Kelimeler

17-α-Etinilestradiol, moleküler baskılanmış polimer, yüzey plazmon rezonans, kuartz kristal mikrobalans.

Article History: Received: Aug 15, 2024; Accepted: Nov 27, 2024; Available Online: Dec 16, 2024.

DOI: https://doi.org/10.15671/hjbc.1533439

Correspondence to: M. Okan, METU MEMS Center, Ankara, Türkiye.

E-Mail: memi@hacettepe.edu.tr

INTRODUCTION

Estradiol is a crucial steroid hormone within the estrogen group, widely recognized for its essential role in female reproductive functions. However, its importance extends beyond human physiology. While estradiol regulates critical processes like secondary sexual characteristics, reproductive organ maintenance, and pregnancy in humans, abnormal estradiol levels—either elevated or diminished—can lead to serious health conditions. These include breast cancer, weight fluctuations, irregular menstrual cycles, osteoporosis, and fertility issues in both men and women [1], [2], [3], [4]. Its importance in medical diagnostics cannot be understated.

Simultaneously, estradiol and its synthetic analogs, such as 17α-ethinyl estradiol (17EE), are increasingly recognized as hazardous environmental pollutants. These compounds belong to the category of endocrine-disrupting chemicals (EDCs), which interfere with the endocrine systems of aquatic organisms, causing reproductive and developmental harm. 17EE, widely used in contraceptives and hormone replacement therapy, often finds its way into the environment through agricultural runoff, sewage, and industrial effluents [5], [6] [7], [8]. Given the dual importance of estradiol in both human health and environmental protection, developing robust, sensitive, and field-deployable biosensors for estradiol detection is a critical scientific goal.

Traditional methods for detecting estradiol, including gas chromatography-mass spectrometry (GC-MS), high-performance liquid chromatography (HPLC), and liquid chromatography-mass spectrometry (LC-MS), offer high sensitivity and specificity [9] [10], [11], [12]. However, these techniques come with significant drawbacks—they are labor-intensive, costly, time-consuming, and require highly skilled operators. The need for faster, more cost-effective methods is particularly pressing in contexts like environmental monitoring, where timely detection of contaminants can prevent ecosystem damage, and in healthcare, where real-time hormone monitoring could improve personalized treatments.

Biosensors based on molecularly imprinted polymers (MIPs) offer a promising solution to these challenges. MIPs are artificial polymers engineered with specific binding sites tailored to the size, shape, and chemical properties of a target molecule [13], [14]. These sites are formed by polymerizing functional monomers in the presence of a template compound—such as 17EE—which is then removed to leave behind complementary binding sites. MIPs have been widely applied in fields such as drug delivery [15], bioassays [16], and as recognition elements in biosensors [17] [18], [19]. Their ability to selectively bind target molecules, coupled with their robustness, makes MIPs ideal for use in field-deployable sensors that require minimal maintenance and high durability.

In this study, we aimed to fill a gap in the literature by focusing on 17EE-imprinted MIPs, rather than the more commonly studied 17β-estradiol and estrone and investigating their performance in two biosensing platforms: Surface Plasmon Resonance (SPR) and Quartz Crystal Microbalance (QCM). SPR sensors, although not mass-based, provide insight into molecular binding events by measuring changes in the refractive index of the sensor's surface [20]. QCM sensors, on the other hand, function as nanogram-level mass-based detectors that monitor changes in frequency due to analyte binding [21] [22] . By utilizing both platforms, we aimed to cross-validate the performance of the 17EE-MIPs, providing a comprehensive analysis of their binding affinity and sensitivity to low concentrations of 17EE.

While there have been studies on hormone detection using 17β-estradiol-imprinted MIPs [23] and estrone-imprinted MIPs [24], this study is the first to employ 17EE-imprinted MIPs in both SPR and QCM systems. The results from this work demonstrate that MIPs are a viable and highly sensitive option for detecting 17EE in both environmental and clinical samples, paving the way for future biosensor development and broader application of this technology.

MATERIALS and METHODS

Materials

17α-ethinyl estradiol (17EE), β-estradiol, estriol, polyvinyl alcohol (PVA), sodium dodecyl sulfate (SDS), methacrylic acid (MAA), ethylene glycol dimethacrylate (EGDMA), 2-hydroxyethyl methacrylate (HEMA), ethanol, (3-aminopropyl)triethoxysilane (APTES), triethylamine (TEA), sodium hydroxide (NaOH), 2-morpholinoethanesulphonic acid (MES), 1-ethyl-3-(3-dimethylaminopropyl)carbodiimide (EDC) and *N*-Hydroxysuccinimide (NHS) were purchased from Sigma Aldrich, Germany.

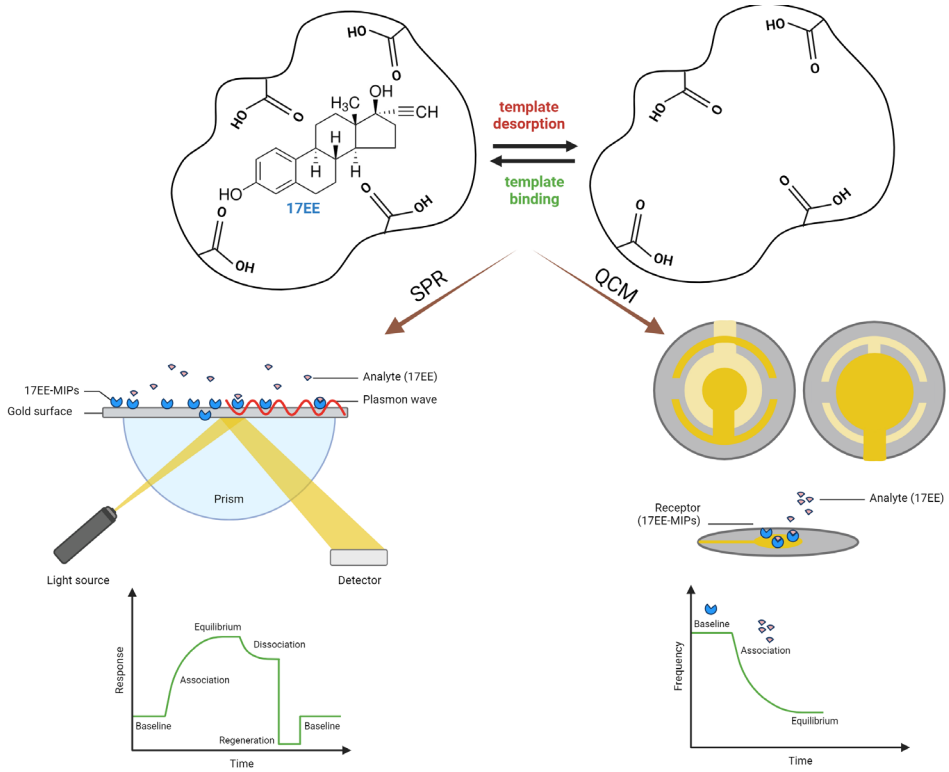

Figure 1. Overall scheme of the study.

Synthesis of 17EE imprinted polymeric nanoparticles

For the synthesis of 17EE-MIP nanoparticles mini-emulsion polymerization technique was employed. For this synthesis three aqueous phases were prepared. The first aqueous phase contains 93.75 mg PVA, 14.425 mg SDS and 11.725 mg sodium bicarbonate in 5 mL DI water. The second aqueous phase contains 50 mg PVA and 50 mg SDS in 100 mL DI water. The third phase is called the oil phase and includes 100 µM 17EE, 254.1 µL functional monomer MAA, 1.05 mL crosslinker EGDMA and 225 µL co-monomer HEMA. Firstly, the oil phase is mixed with the first aqueous phase and homogenized at 25000 rpm. The mixture is then added to the second aqueous phase under stirring at 600 rpm with magnetic stirrer and heated to 40°C. Finally, initiator pair of 125 mg sodium bisulfate and 125 mg ammonium persulfate are added, and the polymerization is let to take place for the following 24 h. Once the polymerization was completed, un-polymerized monomers together with other leftover chemicals were washed by centrifuging at 26500 rpm for 1h. The washing was repeated with DI water-ethanol (1:1, v/v) mixture 5 times and with bare DI water twice. The synthesized 17EE-MIPs were stored at 4°C.

Surface modification of SPR and QCM chips

To immobilize synthesized 17EE-MIPs on gold surface, gas phase amination was performed in a desiccator under Argon using 30 µM APTES and 10 µM TEA. After 2 h, APTES and TEA were removed from the desiccator and surfaces were let to cure under argon for 2 days. Free carboxyl functional groups (COOH) within 17EE-MIPs were covalently bound to amine groups (NH_2) created on the gold surface using carbodiimide crosslinking. For this, 10 mM EDC and 10 mM NHS was prepared in 0.1 M MES buffer (at pH 4.7). The solution was initially incubated with 17EE-MIPs (45 min) to activate the carboxyl groups, followed by surface treatment to complete the crosslinking process (2 h). The crystals were washed with DI water to remove non-crosslinked molecules and non-specifically attached species.

SPR studies

After being activated with buffer solution (for 5 mins), the 17EE solution was passed through until re-equilibrium was reached (for ~10 mins). Finally, 17EE sensorgrams were obtained using desorption solution (for ~ 5 mins). Approximately 20 mins were waited for both binding and regeneration stages in all measurements. During SPR measurements SPR Mini (Nanodev, Ankara, Turkey) was used.

Equilibrium & binding kinetics analysis and isotherm models

Equilibrium analysis

If the total ligand concentration ($[B]_0$) is defined as the maximum analyte binding capacity of the surface; then all other concentration values can be expressed as SPR signals. Thus, there is no need to convert mass to concentration. Under pseudo-first-order conditions where the free analyte concentration remains constant in the flow cell, binding is expressed as follows:

$$d\Delta R/dt = k_a C\Delta R_{max} - (k_a C + k_d)\Delta R \quad \text{Equation 1}$$

Here, $d\Delta R/dt$ is the rate of change of the SPR signal, m and ΔR_{max} represent the maximum signal measured from binding and resulting from mass increase (nM/cm^2), C is the analyte concentration (nM), k_a is the association rate constant (nM/s), and k_d is the dissociation constant (1/s). The binding constant K_A (nM) is calculated from the ratio of k_a and k_d constant ($K_A=k_a/k_d$). At equilibrium, the equation is simplified by setting $d\Delta R/dt=0$.

$$\Delta m_{equilibrium}/C = K_A\Delta m_{max} - K_A\Delta m_{equilibrium} \quad \text{Equation 2}$$

Hence, the binding constant K_A is calculated from the $\Delta m_{equilibrium}/C$ versus $\Delta m_{equilibrium}$ graph. The dissociation constant KD can be calculated using the equation $1/K_A$.

Binding kinetic analysis

When Equation 2 is re-arranged, Equation 1 can be obtained. The graph of $d\Delta R/dt$ versus ΔR for interaction-controlled kinetics yields a straight line with a slope of $-(k_a C+k_d)$. The initial binding rate is linearly related to the analyte concentration and is used quantitatively to determine the concentration. If the ΔR_{max} value is known, k_a and k_d values can be calculated using a single sensogram. It is difficult to experimentally determine ΔR_{max} as very high analyte concentrations are required to saturate the surface completely. The preferred approach is to ontain binding sensograms at different analyte concentrations. Graphs of $d\Delta R/dt$ versus ΔR for analysis of forward and reverse rates provide a slope (S) associated with forward and reverse rate constants:

$$S = k_a C + k_d \quad \text{Equation 3}$$

The graph against C for S yields a straight line with a slope of k_a. Theoretically the intersection point gives the k_d value. However, this method is not very reliable for calculating k_d when $k_a C \gg k_d$. A more reliable method is to examine the dissociation kinetics:

$$\ln(\Delta R_0/\Delta R_t) = k_d(t-t_0) \quad \text{Equation 4}$$

where ΔR_0 and ΔR_t are the SPR signal values at different times t_0 and t in the dissociation curve.

Equilibrium isotherm models

Four different isotherm models were applied to determine the interaction model between the suppressed SPR sensor and the template molecule:

Scatchard, Langmuir, Freundlich, and Langmmuir-Freundlich.

Scatchard $\Delta R_{equilibrium}/[C] = K_A(\Delta R_{max} - \Delta R_{equilibrium})$

Langmuir $\Delta R = \{\Delta R_{max}[C]/(K_D+[C])\}$

Freundlich $\Delta R = \Delta R_{max}[C]1/n$

Langmuir-Freundlich $\Delta R = \{\Delta R_{max}[C]1/n/K_D+[C]1/n\}$

where ΔR_{max} is the maximum SPR signal shift, $\Delta R_{equilibrium}$ is the SPR signal shift at equilibrium, [C] is the analyte concentration (μM), K_A (μM) is the binding equilibrium constant, K_D (1/μM) is the dissociation equilibrium constant, 1/n is the Freundlich surface heterogeneity index.

QCM studies

QCM studies were performed in a similar manner to SPR studies. The difference lies in the consecutive nature of the QCM trials where different concentrations of 17EE were introduced to the system consecutively without regeneration steps. During QCM measurements, in house developed liquid chamber by Johannes Kepler University, Linz, Austria was used.

RESULTS and DISCUSSION

Characterization of 17EE imprinted polymeric nanoparticles

Structural characterization of the 17EE-MIPs was carried out with Scanning Electron Microscopy (SEM) (Zeiss EVO 50, Germany). According to SEM analysis, the average sizes of 17EE-MIPs fall within the range of 90-100 nm (Figure 2a). As evident from SEM images, the synthesized particles are homogeneous, uniform in size, and successfully immobilized onto surfaces in a single-layer format. The Fourier-Transform Infrared Spectroscopy (FTIR) (Thermo Fisher Scientific, Nicolet iS10, Walt-

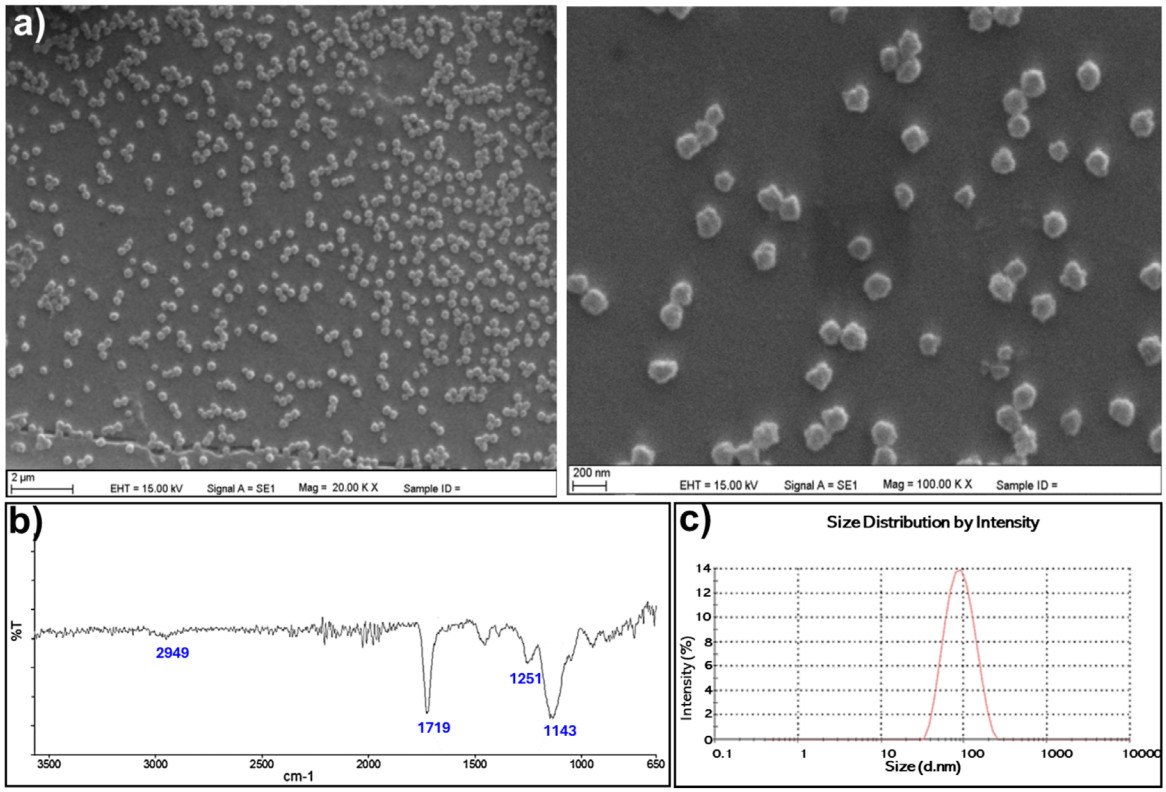

Figure 2. a) SEM images, b) FTIR spectrum and c) zetasizer analysis of the synthesized 17EE-MIPs.

ham, MA, USA) analysis was performed to confirm the chemical composition of the synthesized 17EE-MIP. The spectra (Figure 2b) yielded a CH stretching band at 2949 cm^{-1} and C=O stretching band at 1719 cm^{-1} representing methyl and carbonyl group of MAA and EGDMA, respectively, C-O stretching band at 1251 cm^{-1} representing carboxyl group of MAA and C-O stretching band at 1143 cm^{-1} representing ester group of EGDMA. The peaks in the spectrum confirmed the inclusion of MAA monomers in the 17EE-MIP structure.

The size distribution analysis was conducted for further structural characterization via Nano Zetasizer (NanoS, Malvern Instruments, London, UK), using samples containing a sufficient density of particles in a volume of 3 mL. The measurements were repeated three times, and the results were examined with the software of zeta sizer analyzer, and reported in Figure 2c. The sizes of 17EE-MIPs were determined to be 94.54 nm. The polydispersity value of the prepared particles was measured as 0.133.

SPR studies

The sensorgrams obtained by applying 17EE solutions prepared at different concentrations to the sensor are given in Figure 3a. Initially, the system was allowed to equilibrate with the buffer solution for approximately 5 mins, then the 17EE solution was passed through the system until equilibrium was re-established (approx. 10 mins). Finally, sensorgrams were obtained using desorption solution (approx. 5 mins). The 17EE solutions were prepared in pure water in the presence of 20% 2 M NaOH. 2 M NaOH solution was used as the desorption agent, and the equilibrium solution was prepared with pure water containing 20% 2 M NaOH. ΔR values increased proportionally with increasing concentration. When the data obtained for the range of 5-50 µg/mL (16.8-158.9 µM) were evaluated, the equation of the obtained line (y=0.0154x+0.1481) and linearity (R^2) were calculated as 0.9798, indicating that the prepared SPR sensor measures with 97% linearity within the given concentration range. The limit of detection (LOD) of the system was calculated from 3.3σ/S, where σ represents the blank measurement and S is the slope of the calibration curve and found as 11.57 µM (~3.43 ppm).

Equilibrium & binding kinetic analysis and isotherm models

The Langmuir adsorption model is based on homogeneous, and the Freundlich adsorption model is based on heterogeneous binding assumptions. The Langmuir model has been widely used for binding isotherms using MIPs. However, it has been reported that MIPs include heterogeneous binding regions. The Freundlich adsorption model is particularly suitable for MIP systems at low concentrations. Nonetheless, this model shows some deviations at high concentrations. The Langmuir-Freundlich binary model can be used to prevent these deviations. It has been reported that the Freundlich isotherm can be widely used to measure the heterogeneity of MIPs. MIPs contain a distribution of binding regions for affinity and selectivity. The primary source of heterogeneity in non-covalent MIPs is the formation of incomplete monomer-template molecule structures in the polymerization mixture. The high heterogeneity distribution processed by MIPs increases the number of high-affinity binding regions. Studies have reported that heterogeneity is a key feature of MIPs, and moreover, heterogeneity is an excellent measure of the effectiveness of suppression [27]. The Langmuir Freundlich and Langmuir-Freundlich parameters were calculated from the expression given in Section 2.5 and presented in Table 1. The data obtained experimentally is compatible with the Freundlich model (R^2=0.9934).

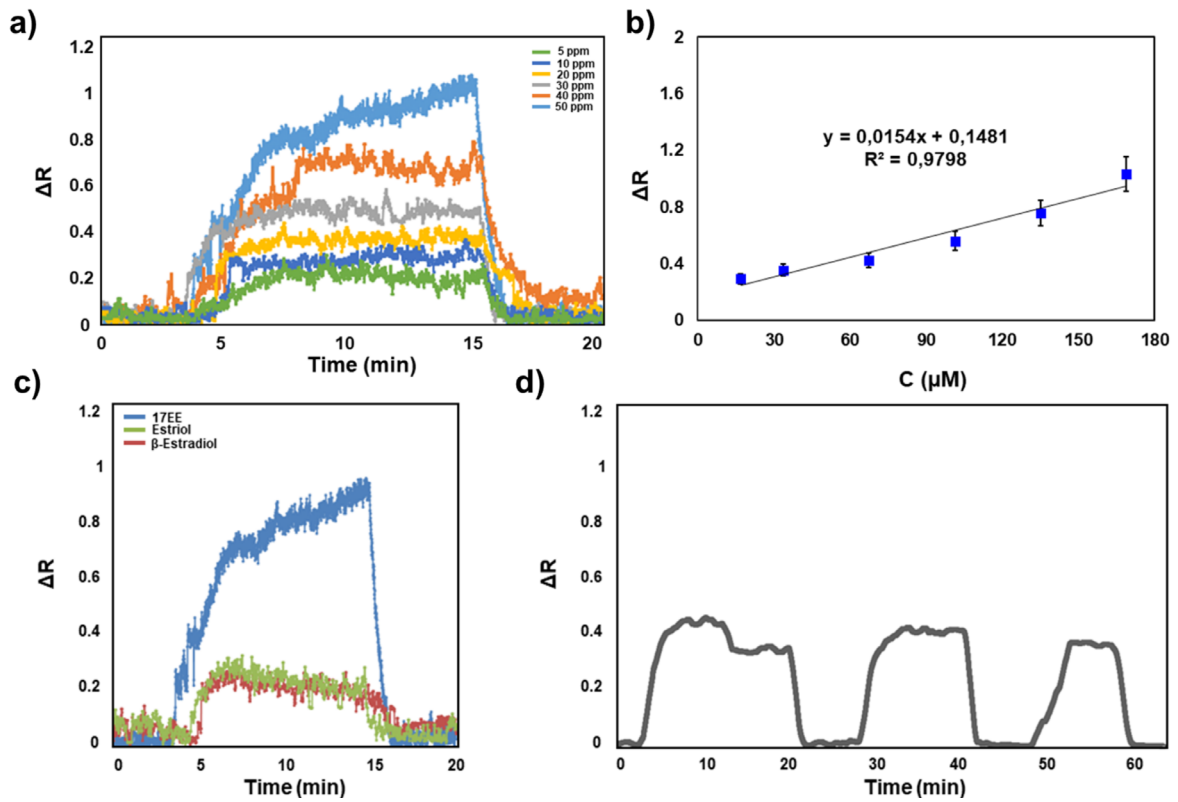

Figure 3. a) SPR sensorgram for different concentrations of 17EE, b) calibration curve derived from sensorgram, c) selectivity of the sensor by comparing same concentrations (50 ppm) of 17EE with estriol and β-estradiol and d) repeatability of the system (with 30 ppm 17EE).

Table 1. Calculated parameters of the different isotherm models.

Langmuir	Freundlich	Langmuir-Freundlich
ΔRmax 0.7833	ΔRmax 2.0081	ΔRmax 2.5107
K_A 19.170	1/n 0.6972	K_A 0.7030
K_D 0.0522		K_D 1.4225
R^2 0.9765	R^2 0.9934	R^2 0.9825

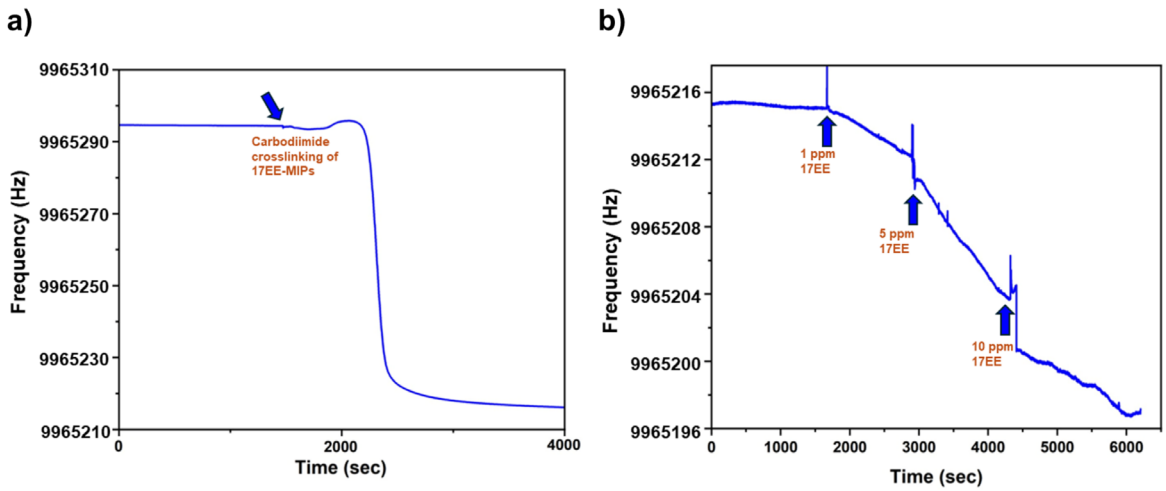

Figure 4. a) Real time frequency drop during 17EE-MIP immobilization on QCM crystal, b) consecutive binding analysis using 3 17EE-MIP concentrations and corresponding frequency changes.

Consecutive QCM studies

Initially, QCM crystal's frequency response during 17EE-MIP immobilization was recorded and given in Figure 4a. The nominal frequency of the crystal was determined as 9.965295 MHz. Once the signal was stable, EDC/NHS activated 17EE-MIPs were introduced to the system with a constant pumping rate of 5 µL/min. Due to large amount of loaded mass on the crystal surface, a significant frequency drop of approximately 75 Hz was observed. Consecutive measurement with QCM was carried out by introducing 3 different concentrations, namely 1 ppm (3.4 µM), 5 ppm (16.9 µM) and 10 ppm (33.7 µM) to the system, starting from lowest to highest. No regeneration was performed between steps. 1, 5 and 10 ppm of 17EE exposure resulted in averaged frequency decreases of 3, 11 and 18 Hz (n=3), with standard deviations of 0.5, 0.5 and 1.3 Hz, respectively. The linear line of the calibration curve has the equation y=1.6557x+1.8361 and R^2 value of 0.9895, yielding very high linearity. The σ of the system was 0.67 Hz and the LOD was calculated using the same equation explained under section 3.2 and found as 1.335 µM (0.396 ppm).

The QCM sensor demonstrated a lower LOD of 1.335 µM, in contrast to the SPR sensor, which exhibited an LOD of 11.57 µM. Despite both sensors utilizing 17EE-MIPs, the QCM sensor's superior sensitivity can be attributed to its unique detection mechanism and inherent properties. QCM sensors operate by measuring frequency changes resulting from mass variations on the sensor surface. This detection method is highly sensitive to small mass changes, as the QCM technique directly translates mass accumulation into a measurable frequency shift. The 17EE-MIPs enhance the specific binding of 17EE, leading to precise and significant mass changes on the sensor surface, thus yielding a lower LOD. The high sensitivity of QCM to mass changes, even at very low analyte concentrations, enables more effective detection. On the other hand, SPR sensors detect changes in the refractive index near the sensor surface. While SPR provides powerful real-time, label-free detection capabilities, its sensitivity can be influenced by several factors. The primary limitation arises from the relatively smaller changes in the refractive index induced by the binding of analytes, particularly at low concentrations. This refractive index change may not be as pronounced as the mass change detected by QCM, resulting in a higher LOD. Additionally, the sensitivity of SPR can be affected by the optical properties of the medium and the efficiency of the plasmonic resonance, which may further limit its performance in detecting lower analyte concentrations. Therefore, the superior sensitivity and lower LOD of the QCM sensor, despite using the same MIPs as the SPR sensor, can be attributed to the QCM's direct and highly sensitive detection of mass changes, compared to the more limited refractive index changes measured by SPR.

In a study conducted by Aylaz and Andaç [28], Equilin (Equ), which is an estrogenic hormone, was detected via QCM based on affinity-recognition-based interactions using amino acids. Low LOD values were obtained, varying from the amino acid used. They have successfully studied within the concentration range of 25-500 nM. It

was found that selected amino acid's hydrophobic residues aligned with the Equ ring system, suggesting that these hydrophobic interactions play a role in the binding process. Although basic amino acids are not prohibitively expensive, specialized or purified amino acids can be more costly. One other point is that the shelf-life of amino acids varies depending on storage conditions, purity and chemical stability. In this sense, MIPs introduce a low-cost and highly stable solution, making them an optimum tailored recognition element. In a study by Minopoli et al. [29], a sensitive immunosensor was developed based on Localized SPR (LSPR) for β-estradiol. The system contains gold nanoparticles (AuNPs) conjugated with antibodies. Although their system was found to have a very low detection limit of 11 pM (3 pg/mL), similarly, employment of antibodies introduces high-cost and low-stability issues. Another crucial point is that the primary performance of an immunosensor is predominantly determined by the antibody choice, the technique employed for antibody fixation and the biological marker utilized to mark the antibody for system detection. The stability and sensitivity of such systems are greatly influenced by factors such as the quantity of immune molecules affixed to the surface, their structural stability and their arrangement on the sensor's surface [30]. All these parameters need detailed and long investigations and optimization studies. Estradiol biosensors employing enzymes as bioreceptors are frequently integrated with electrochemical techniques [31]. Their effectiveness relies on the characteristics and arrangement of the enzymes used, as well as the surface properties and structure of the electrodes. The enzyme that is immobilized must not only securely attach to the electrode surface but also preserve its biological functionality [32]. In the study conducted by Jijana [33], Horseradish Peroxide (HRP) was used as a bioreceptor to detect estradiol. She utilized a nanocomposite embedded within polyaniline to immobilize HRP on the surface of the gold electrode through entrapment. The developed sensor demonstrated precise and effective measurement of estradiol concentrations ranging from 0.2 to 4 µM, with an LOD of 0.2 µM. Compared with this particular study, the system proposed in this paper contains a rather straightforward and easy-to-perform surface modification approach, in the meanwhile eliminating the need for complex nanostructures and biological components.

Table 2 summarizes the published studies in the field on sensors for the detection of 17β-estradiol, a natural estrogen hormone. Since 17EE is a synthetic derivative of estradiol and a modified version of this natural hormone, the published studies on 17β-estradiol detection provide the closest comparisons available. All studies presented in Table 2 involve electrochemical detection methods with MIPs. To the best of our knowledge, however, our study is the first to focus on the detection of 17α-ethinyl estradiol using SPR and QCM techniques. This novel approach expands the field by introducing SPR and QCM platforms for detecting synthetic estrogens, demonstrating the unique advantage of MIPs in selectivity and sensitivity for synthetic hormone detection, which can be crucial in environmental and clinical applications.

CONCLUSION

This study demonstrates the superior sensitivity of the QCM sensor over the SPR sensor for detecting 17EE using imprinted polymeric nanoparticles. The QCM sensor achieved a significantly lower LOD of 1.335 µM compared to the SPR sensor's LOD of 11.57 µM. This enhanced sensitivity is attributed to the QCM's mass-based detection mechanism. The synthesized 17EE-MIPs facilitate specific and efficient binding of 17EE, resulting in precise mass changes that are easily detected by the QCM sensor. In contrast, the SPR sensor, which relies on refractive index changes, is inherently less sensitive to

Table 2. Table of published sensor studies that employed MIPs for similar hormone detection.

Analyte	Technique	Additional Materials	LOD	Reference
17β-estradiol	Electrochemistry	Multi-walled carbon nanotubes and gold nanoparticles	$2.5x10^{-16}$ M	[34]
17β-estradiol	Electrochemistry	Magnetic particles	0.13 µM	[35]
17β-estradiol	Electrochemistry	Carbon black	0.03 µM	[36]

small analyte concentrations, particularly at low levels. Factors such as the limited refractive index change and the influence of optical properties and plasmonic resonance efficiency contribute to the higher LOD observed in the SPR sensor. The findings highlight the advantages of using QCM sensors with MIPs for highly sensitive detection of estrogenic compounds, offering a cost-effective and stable alternative to other sensing methods that rely on more complex biological components.

The findings of this study hold significant promise for both environmental and clinical applications. In the context of environmental diagnostics, the detection of EDCs such as 17EE in wastewater is of critical importance due to the detrimental effects these compounds can have on aquatic ecosystems and wildlife. Traditional methods for detecting EDCs in environmental samples, such as chromatography-based techniques, though effective, are often time-consuming and require expensive equipment and highly skilled personnel. The 17EE- MIPs developed in this study, coupled with SPR and QCM biosensor platforms, provide a rapid, cost-effective, and highly sensitive alternative for in-field environmental monitoring. These sensors have the potential to be integrated into automated, portable devices that could be deployed to continuously monitor water sources for contamination, ensuring timely detection of EDCs and allowing for faster remediation efforts.

In the realm of clinical diagnostics, the ability to accurately monitor estradiol levels is crucial for managing conditions such as hormone imbalances, infertility, menopause, and certain cancers. The highly sensitive detection limits achieved in this study suggest that the 17EE-MIP-based sensors could be adapted for point-of-care testing (POCT) devices in healthcare settings. These sensors could offer a non-invasive, real-time monitoring solution for patients undergoing hormone therapy or for those requiring regular estradiol level assessments. Such devices would improve patient outcomes by enabling faster diagnosis and more personalized treatment strategies, as opposed to relying solely on laboratory-based assays which involve lengthy processing times.

Acknowledgments

This research was supported by The Scientific and Technological Research Council of Turkey (TÜBİTAK, Project No: 113Z222). The authors thank Dr. Esma Sari for her contributions in the SPR measurements and kinetic analysis.

References

1. P. P. Waifalkar, D. Noh, P. Derashri, S. Barage, and E. Oh, 'Role of Estradiol Hormone in Human Life and Electrochemical Aptasensing of 17β-Estradiol: A Review', Dec. 01, 2022, MDPI. doi: 10.3390/bios12121117.
2. H. Seeger, F. P. Armbruster, A. O. Mueck, and T. H. Lippert, 'The effect of estradiol on urodilatin production in postmenopausal women', 1998.
3. M. K. L. Coelho, D. N. da Silva, and A. C. Pereira, 'Development of electrochemical sensor based on carbonaceal and metal phthalocyanines materials for determination of ethinyl estradiol', Chemosensors, vol. 7, no. 3, Sep. 2019, doi: 10.3390/CHEMOSENSORS7030032.
4. W. Rosner, S. E. Hankinson, P. M. Sluss, H. W. Vesper, and M. E. Wierman, 'Challenges to the measurement of estradiol: An endocrine society position statement', Journal of Clinical Endocrinology and Metabolism, vol. 98, no. 4, pp. 1376–1387, Apr. 2013, doi: 10.1210/jc.2012-3780.
5. X. Yang et al., 'Occurrence and distribution of natural and synthetic progestins, androgens, and estrogens in soils from agricultural production areas in China', Science of the Total Environment, vol. 751, Jan. 2021, doi: 10.1016/j.scitotenv.2020.141766.
6. Y. Q. Liang et al., 'The progestin norethindrone alters growth, reproductive histology and gene expression in zebrafish (Danio rerio)', Chemosphere, vol. 242, Mar. 2020, doi: 10.1016/j.chemosphere.2019.125285.
7. A. Di Nisio et al., 'Perfluorooctanoic acid alters progesterone activity in human endometrial cells and induces reproductive alterations in young women', Chemosphere, vol. 242, Mar. 2020, doi: 10.1016/j.chemosphere.2019.125208.
8. J. O. Ojoghoro, M. D. Scrimshaw, and J. P. Sumpter, 'Steroid hormones in the aquatic environment', Oct. 20, 2021, Elsevier B.V. doi: 10.1016/j.scitotenv.2021.148306.
9. L. Martín-Pozo, M. D. C. Gómez-Regalado, I. Moscoso-Ruiz, and A. Zafra-Gómez, 'Analytical methods for the determination of endocrine disrupting chemicals in cosmetics and personal care products: A review', Nov. 01, 2021, NLM (Medline). doi: 10.1016/j.talanta.2021.122642.
10. Y. Yang, J. Chen, and Y. P. Shi, 'Determination of diethylstilbestrol in milk using carbon nanotube-reinforced hollow fiber solid-phase microextraction combined with high-performance liquid chromatography', Talanta, vol. 97, pp. 222–228, Aug. 2012, doi: 10.1016/j.talanta.2012.04.021.
11. R. Mesa, A. Kabir, V. Samanidou, and K. G. Furton, 'Simultaneous determination of selected estrogenic endocrine disrupting chemicals and bisphenol A residues in whole milk using fabric phase sorptive extraction coupled to HPLC-UV detection and LC-MS/MS', J Sep Sci, vol. 42, no. 2, pp. 598–608, Jan. 2019, doi: 10.1002/jssc.201800901.
12. H. Zhang, Z. Cui, B. Yang, D. Fang, Y. Liu, and Z. Wang, 'Integrated recombinant gene yeast bioassay and HPLC-MS analysis for detection of low-dose multi-component residue of hormone-like compounds in environment', Science of the Total Environment, vol. 773, Jun. 2021, doi: 10.1016/j.scitotenv.2021.145569.
13. L. Chen, S. Xu, and J. Li, 'Recent advances in molecular imprinting technology: Current status, challenges and highlighted applications', Chem Soc Rev, vol. 40, no. 5, pp. 2922–2942, Apr. 2011, doi: 10.1039/c0cs00084a.

14. G. Vasapollo et al., 'Molecularly imprinted polymers: Present and future prospective', Sep. 2011. doi: 10.3390/ijms12095908.
15. B. T. S. Bui and K. Haupt, 'Molecularly imprinted polymers: Synthetic receptors in bioanalysis', Nov. 2010. doi: 10.1007/s00216-010-4158-x.
16. Y. Hoshino et al., 'Recognition, neutralization, and clearance of target peptides in the bloodstream of living mice by molecularly imprinted polymer nanoparticles: A plastic antibody', J Am Chem Soc, vol. 132, no. 19, pp. 6644–6645, May 2010, doi: 10.1021/ja102148f.
17. Y. Ge and A. P. F. Turner, 'Molecularly imprinted sorbent assays: Recent developments and applications', Aug. 17, 2009. doi: 10.1002/chem.200802401.
18. D. Udomsap et al., 'Electrochemical molecularly imprinted polymers as material for pollutant detection', Mater Today Commun, vol. 17, pp. 458–465, Dec. 2018, doi: 10.1016/j.mtcomm.2018.10.019.
19. S. Lépinay, K. Kham, M. C. Millot, and B. Carbonnier, 'In-situ polymerized molecularly imprinted polymeric thin films used as sensing layers in surface plasmon resonance sensors: Mini-review focused on 2010-2011', May 2012. doi: 10.2478/s11696-012-0134-6.
20. J. Homola and M. Piliarik, 'Surface Plasmon Resonance (SPR) Sensors', in Surface Plasmon Resonance Based Sensors, Springer, 2006, ch. 2, pp. 45–67.
21. J. Homola, 'Present and future of surface plasmon resonance biosensors', Oct. 2003. doi: 10.1007/s00216-003-2101-0.
22. D. Battal, S. Akgönüllü, M. S. Yalcin, H. Yavuz, and A. Denizli, 'Molecularly imprinted polymer based quartz crystal microbalance sensor system for sensitive and label-free detection of synthetic cannabinoids in urine', Biosens Bioelectron, vol. 111, pp. 10–17, Jul. 2018, doi: 10.1016/j.bios.2018.03.055.
23. S. Klangprapan, B. Choke-arpornchai, P. A. Lieberzeit, and K. Choowongkomon, 'Sensing the classical swine fever virus with molecularly imprinted polymer on quartz crystal microbalance', Heliyon, vol. 6, no. 6, Jun. 2020, doi: 10.1016/j.heliyon.2020.e04137.
24. A. G. Ayankojo, J. Reut, R. Boroznjak, A. Öpik, and V. Syritski, 'Molecularly imprinted poly(meta-phenylenediamine) based QCM sensor for detecting Amoxicillin', Sens Actuators B Chem, vol. 258, pp. 766–774, Apr. 2018, doi: 10.1016/j.snb.2017.11.194.
25. U. Latif, J. Qian, S. Can, and F. L. Dickert, 'Biomimetic receptors for bioanalyte detection by quartz crystal microbalances — from molecules to cells', Sensors (Switzerland), vol. 14, no. 12, pp. 23419–23438, Dec. 2014, doi: 10.3390/s141223419.
26. J. Liu et al., 'Study on the Preparation of Estrone Molecularly Imprinted Polymers and Their Application in a Quartz Crystal Microbalance Sensor via a Computer-Assisted Design', Int J Mol Sci, vol. 23, no. 10, May 2022, doi: 10.3390/ijms23105758.
27. E. Sari, R. Üzek, M. Duman, and A. Denizli, 'Fabrication of surface plasmon resonance nanosensor for the selective determination of erythromycin via molecular imprinted nanoparticles', Talanta, vol. 150, pp. 607–614, Apr. 2016, doi: 10.1016/j.talanta.2015.12.043.
28. G. Aylaz and M. Andaç, 'Affinity-Recognition-Based Gravimetric Nanosensor for Equilin Detection', Chemosensors, vol. 10, no. 5, May 2022, doi: 10.3390/chemosensors10050172.
29. A. Minopoli et al., 'LSPR-based colorimetric immunosensor for rapid and sensitive 17β-estradiol detection in tap water', Sens Actuators B Chem, vol. 308, Apr. 2020, doi: 10.1016/j.snb.2020.127699.
30. A. Makaraviciute and A. Ramanaviciene, 'Site-directed antibody immobilization techniques for immunosensors', Dec. 15, 2013. doi: 10.1016/j.bios.2013.06.060.
31. X. Wang et al., '17β-estradiol biosensors based on different bioreceptors and their applications', 2024, Frontiers Media SA. doi: 10.3389/fbioe.2024.1347625.
32. H. H. Nguyen, S. H. Lee, U. J. Lee, C. D. Fermin, and M. Kim, 'Immobilized enzymes in biosensor applications', Jan. 02, 2019, MDPI AG. doi: 10.3390/ma12010121.
33. A. N. Jijana, 'Polyaniline Entrapped Water-Dispersible 3MPA-ZnSe Quantum Dots and Their Application for the Development of an Enzymatic Electrochemical Nanobiosensor for the Detection of 17β-Estradiol, an Endocrine-Disrupting Compound', Appl Biochem Biotechnol, vol. 195, no. 5, pp. 3425–3455, May 2023, doi: 10.1007/s12010-022-04277-w.
34. D. Futra, L. Y. Heng, M. Z. Jaapar, A. Ulianas, K. Saeedfar, and T. L. Ling, 'A novel electrochemical sensor for 17β-estradiol from molecularly imprinted polymeric microspheres and multi-walled carbon nanotubes grafted with gold nanoparticles', Anal. Methods, vol. 8, no. 6, pp. 1381-1389, Jan. 2016.
35. D. N. da Silva and A. C. Pereira, 'Development of a Chemically Modified Electrode with Magnetic Molecularly Imprinted Polymer (MagMIP) for 17β-Estradiol Determination in Water Samples', Electrochem, vol. 3, no. 4, pp. 809-819, Dec. 2022.
36. D. N. da Silva and A. C. Pereira, 'An electrochemical sensor modified with a molecularly imprinted polymer and carbon black for 17β-estradiol detection', Anal. Methods, vol 14., no. 12, pp. 1208-1213, Mar. 2022.